Available online at www.sciencedirect.com
ScienceDirect
Physics Letters A 359 (2006) 295–299
PHYSICS LETTERS A
www.elsevier.com/locate/pla

Spin polarization and transport in the manganite $La_{0.85}Te_{0.15}Mn_{0.9}Cu_{0.1}O_3$

R. Ang *, Y.P. Sun *, J. Yang, X.B. Zhu, W.H. Song

Key Laboratory of Materials Physics, Institute of Solid State Physics, and Hefei High Magnetic Field Laboratory, Chinese Academy of Sciences, Hefei 230031, People's Republic of China

Received 25 April 2006; received in revised form 13 May 2006; accepted 16 May 2006

Available online 23 June 2006

Communicated by R. Wu

Abstract

The resistivity $\rho(T)$, and thermoelectric power (TEP) $S(T, H)$ in the manganite $La_{0.85}Te_{0.15}Mn_{0.9}Cu_{0.1}O_3$ have been investigated systematically in the absence and presence of magnetic fields. A large negative magnetoresistance (MR) appears up to 5 T. In addition, $S(T)$ of the sample shows an anomalous peak, which is suggested to be related to the contribution of phonon drag. Particularly, the thermally induced and the field-induced sign change of S below the Curie temperature T_C is observed, implying the importance of spin polarization. In terms of the change of electronic structure, the orbital degree of freedom of the e_g carriers can be responsible for the effective lifting of the degenerate e_g band. Additionally, based on the fitting results of $\rho(T)$ and $S(T)$, the transport mechanism for the sample in the paramagnetic (PM) insulting region and low-temperature ferromagnetic (FM) insulating region below T_C is suggested to be dominated by variable-range-hopping (VRH) conduction. However, in the intermediate-temperature FM metallic region below T_C, the transport mechanism is considered to be dominated mainly electron–magnon scattering.

PACS: 75.47.Lx; 72.25.-b

Keywords: Thermoelectric power; Spin polarization; Transport mechanism

1. Introduction

The transport properties of mixed-valent manganites with perovskite structure have received much notice in recent years because of the discovery of colossal magnetoresistance (CMR). Much attention has been paid to the hole-doped manganites $La_{1-x}(Ca, Sr, Ba)_xMnO_3$ due to their potential applications such as magnetic reading heads, field sensors and memories [1]. Their behaviors have been interpreted based on the double-exchange (DE) mechanism [2] and the Jahn–Teller (JT) distortion [3].

Recently, much research has also placed on emphasis on the electron-doped manganites $La_{1-x}(Ce, Zr, Te)_xMnO_3$ because of the interesting applications in the emerging field of spintronics [4]. It is believed that the study of the doping effects at Mn site should provide important clues to the mechanism of CMR behavior because of the core role of Mn ions. Very recently, the effect of the Cu-doping at Mn sites on the electron-type manganites $La_{0.85}Te_{0.15}MnO_3$ is investigated through measuring the electrical transport and magnetic properties in our previous work [5]. Especially for the $La_{0.85}Te_{0.15}Mn_{0.9}Cu_{0.1}O_3$ sample, it is found that the magnetic property occurs a remarkable variation. As we know, thermoelectric power (TEP) S is not affected by the grain boundaries of the polycrystalline sample and is sensitive to the band structure and carrier mobility near the Fermi level. Consequently, in order to further investigate the peculiar character of $La_{0.85}Te_{0.15}Mn_{0.9}Cu_{0.1}O_3$, in this Letter, we measure systemically thermoelectric power (TEP) $S(T, H)$ of the sample in the absence and presence of the applied fields.

2. Experiment

Details of the sample preparation and its characterization by X-ray diffraction, magnetization measurements have been reported in Ref. [5]. The measurements of ρ and S were per-

* Corresponding authors. Tel.: +86 551 559 2757; fax: +86 551 559 1434.
E-mail addresses: rang@issp.ac.cn (R. Ang), ypsun@issp.ac.cn (Y.P. Sun).

0375-9601/$ – see front matter
doi:10.1016/j.physleta.2006.05.093

formed by the standard four-probe method from 5 to 320 K in the absence and presence of magnetic fields using commercial quantum design physical property measurement system (PPMS) ($1.8 \leqslant T \leqslant 400$ K, $0 \leqslant H \leqslant 9$ T). The typical dimension of the measured sample is $8 \times 4 \times 1.2$ mm^3.

3. Results and discussion

The temperature dependence of resistivity $\rho(T)$ of $La_{0.85}Te_{0.15}Mn_{0.9}Cu_{0.1}O_3$ sample at 0, 1, 3, and 5 T is shown in Fig. 1(a), respectively. Fig. 1(a) shows that $\rho(T)$ curve has only one peak which locates at $T_p = 117$ K at zero field. Here T_p is the temperature of metal–insulator transition (MIT), which is believed to reflect the spin-dependent interfacial tunneling due to the difference in magnetic order between surface and core of ferromagnetic (FM) grains. It is worth noting that T_p peak position does not nearly change in the applied magnetic field, which further verifies the unusual origin of T_p peak. In addition, ρ decrease and a large negative MR is observed near T_p especially at 5 T. The MR as a function of temperature is shown in Fig. 1(b). Here, the MR is defined as $\Delta\rho/\rho_H = (\rho_H - \rho_0)/\rho_H$, where ρ_0 is the resistivity at zero field and ρ_H is the resistivity at $H = 1$, 3, and 5 T, respectively. With the increase of the applied magnetic field, the MR peak close to T_p becomes more obvious. The largest negative MR value can reach -320% at 5 T. It is worth noting that the rapid increase of absolute MR in the FM metallic phase is attributed to the suppressed spin fluctuation in the applied field.

As to $S(T)$, a new peak at T_S^g (= 192 K) emerges at zero field as plotted in Fig. 2. Additionally, there is a minimum at T_S^m (= 139 K). In comparison, the Curie temperature T_C is 169 K [5]. An interesting phenomenon is that S rises gradually with decreasing temperatures and another weaker broad peak located at T_S^d (= 57 K) appears, implying that the origin of T_S^d peak is different from that of T_S^g peak. As the temperature is decreased further, the value of S drops sharply (i.e., $S \to 0$ as $T \to 0$), which is suggested to originate from the weak carrier localization effect. The weak localization effect can be also reflected by $\rho(T)$ measurement due to the little upturn of ρ at low temperatures as shown in Fig. 1(a).

In the vicinity of T_S^d peak, i.e., in the intermediate-temperature FM metallic region, it is found that the $S(T)$ data for the sample can be described by power law $T^{3/2}$ [6], which suggests the importance of electron–magnon scattering in FM metallic phase. Interestingly, the gradual increase of $S(T)$ value in the vicinity of T_S^d is observed at 4 T, which is suggested to the enhancement of electron–magnon scattering in the applied field.

For the new peak located at T_S^g in $S(T)$ curve, it is obvious that $S(T)$ exhibits an abnormal metallic-like behavior between T_S^m and T_S^g. In general, the character of $S(T)$ can be qualitatively understood in terms of Mott's formula for the charge contribution to the Seebeck coefficient in metals [7]:

$$S = -\frac{\pi^2}{3}\frac{k_B^2 T}{e}\frac{\sigma'(E_F)}{\sigma(E_F)}, \tag{1}$$

where k_B is Boltzmann's constant, e is the electron's charge, $\sigma(E_F)$ is the conductivity at Fermi level, and σ' stands for $d[\sigma(E)]/dE$. The observed decrease of absolute S below T_S^g can be explained as the increase of conductivity provided that $\sigma' \approx$ const. However, if one assumes σ' is constant and almost isotropic electrical transport properties, i.e., $\sigma^{-1} = \rho$, then according to Eq. (1), $\Delta S/S_0 \propto \Delta\rho/\rho_0$ is expected. The plot of $|\Delta S/S_0|$ vs. $|\Delta\rho/\rho_0|$ for data of $La_{0.85}Te_{0.15}Mn_{0.9}Cu_{0.1}O_3$ is shown in Fig. 3(a), which shows that the data at $T_0 = 150$, 160, 170 and 180 K all evidently deviate from the theoretical prediction of Eq. (1) (linearity). Therefore, the assumption $\sigma' \approx$ const is not reasonable as argued by Uhlenbruck et al. [8]. In other words, the assumption that σ' is constant given by Asamitsu et al. [9] is not valid for the present studied system. An important

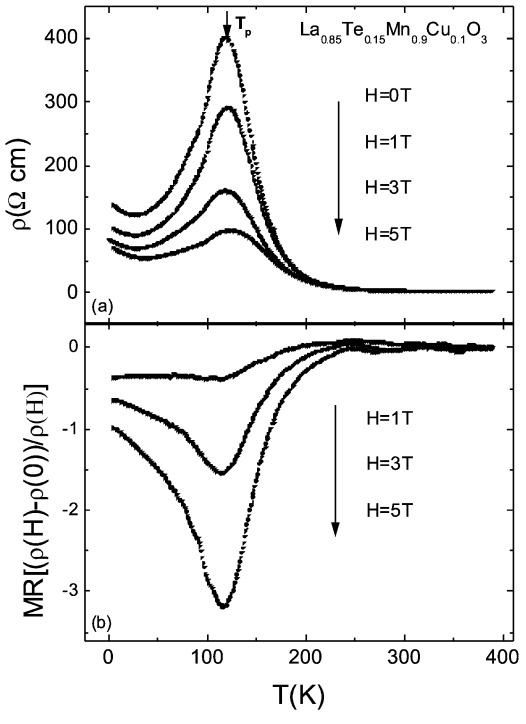

Fig. 1. (a) The temperature dependence of resistivity $\rho(T)$ at 0, 1, 3 and 5 T. (b) MR for $La_{0.85}Te_{0.15}Mn_{0.9}Cu_{0.1}O_3$ sample at 1, 3 and 5 T, respectively.

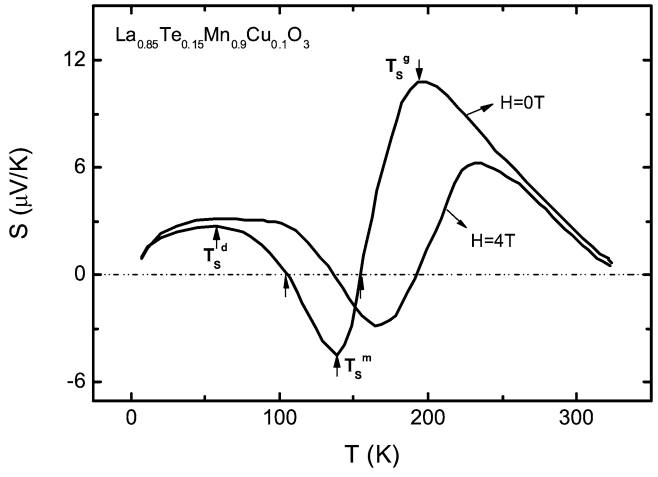

Fig. 2. The temperature dependence of $S(T)$ at 0 and 4 T.

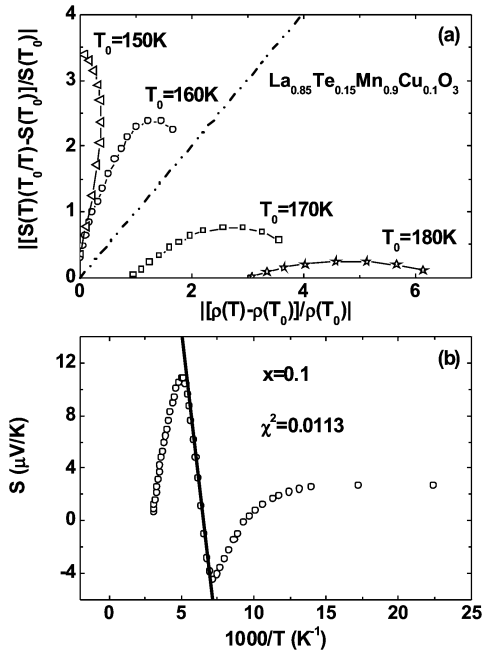

Fig. 3. (a) Relative changes of $S(T)$ vs. relative changes of $\rho(T)$ for the sample ($T_0 = 150$, 160, 170 and 180 K). The dotted line expresses the prediction of Mott's formula with Eq. (1) (see text) and (b) the fitting of $S(T)$ data between T_S^m and T_S^g with Eq. (2) (see text) for $x = 0.10$. The parameter χ^2 (reduced chi-square value of fit) represents the quality of the fit.

contribution to the T_S^g peak may be the phonon drag effect as discussed below.

As we know, according to the theoretical model, the phonon drag TEP S_g can meet following relationship [10]:

$$S_g \propto 1/T. \tag{2}$$

The curve of S vs. $1000/T$ for the sample is plotted in Fig. 3(b). The scatter symbols correspond to the experimental data and the solid lines denote the fitted results according to Eq. (2). The parameter χ^2 (reduced chi-square value of fit) related to the quality of the fit is also shown in Fig. 3(b). The fitting voltage value is -9.6 μV. It is found that the $S_g(T)$ data between T_S^m and T_S^g can be well described by Eq. (2). Hence, the deviation in $|\Delta S/S_0|$ vs. $|\Delta\rho/\rho_0|$ plot (Fig. 3(a)) from the theoretical prediction is due to the presence of considerable phonon drag effect.

In the external magnetic field, the phonon drag effect is expected to become weaker [11], so that the $S(T)$ value reduces. In addition, Fig. 2 exhibits that the applied field makes T_S^d, T_S^m and T_S^p peak positions all shift to higher temperatures. Moreover, the interesting sign change of S is also observed.

In the following, we will focus on analyzing the sign change of S. Fig. 2 displays that S is positive above T_C but changes its sign to negative below T_C. Nevertheless, as $T \ll T_C$, S becomes positive again. The temperature range of $S < 0$ is from 106 to 152 K. If the sign of S reflects a type of charge carriers, the sign change of S suggests that the electronic state of the sample has been altered between electron-like and hole-like charge carriers by lowering the temperatures.

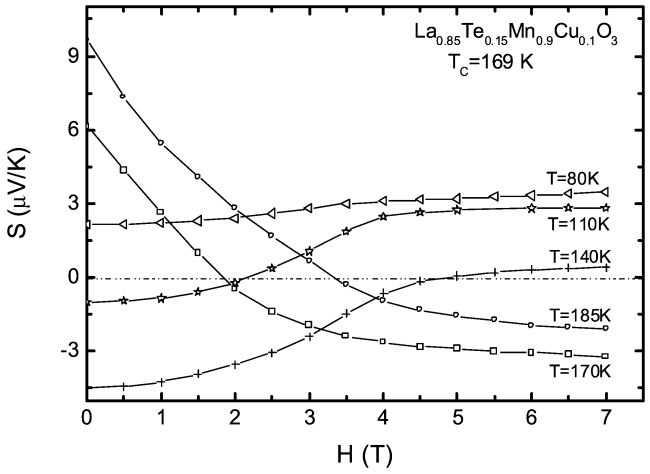

Fig. 4. Magnetic field dependence of $S(H)$ at various temperatures for $La_{0.85}Te_{0.15}Mn_{0.9}Cu_{0.1}O_3$ sample. The arrows denote the sign variation of S.

The thermally induced sign change of S observed for the sample implies that an evolution of spin polarization influences the electronic character of charge carriers. Provided that this is the case, it is expected that the sign change of S can also be induced by the applied magnetic field. Fig. 4 shows the magnetic field dependence of S at different temperatures. As $T > T_C$, the S varies from a positive value to a negative value with increasing applied magnetic fields. As $T < T_C$, the S varies from a negative value to a positive value with increasing applied magnetic fields. Moreover, both issues of $T > T_C$ and $T < T_C$ shows that the magnetic field of the sign change of S increases with increasing temperatures as denoted by arrows. However, as $T \ll T_C$, S has not a sign variation and keeps a positive value.

In order to clarify the above interesting phenomena, it is proposed that the orbital degree of freedom of e_g band may play an important role [12]. As is well known, the e_g band can be built up with degenerate $3d$ orbitals (i.e., $d_{3z^2-r^2}$ and $d_{x^2-y^2}$) and can be split into the upper and the lower band in a certain situation. If the orbital degeneracy is not lifted in crystals, in this instance, it is natural to suppose that the nature of charge carriers is electron type. If the lower (spin-up) band built up with the two orbitals is split further into two bands in the FM state, then the lowest band is fulfilled, the dopants may introduce holes into the system. Thus, we draw a conclusion for the $La_{0.85}Te_{0.15}Mn_{0.9}Cu_{0.1}O_3$ sample, when the temperature is decreased below T_C, the density of states for the lower (upper) spin-up band increases (decreases). As a result, the spin polarization enhances and the degeneracy of the e_g band is gradually lifted. Accordingly, S changes its sign from negative to positive below T_C. But S is only positive at low temperatures, the e_g band in the fully spin-polarized FM state is not degenerate and a further splitting takes place.

However, it is very important and pivotal to confirm what is the driving force for the effective splitting of the fully spin-polarized e_g band. One of the possible origins may be the structural distortion of MnO_6 octahedra or the JT effect. The factor of JT distortion has been recently considered in the theoretical [13] and experimental [14] works to explain the transport properties in the manganese oxides. It can be expected that the

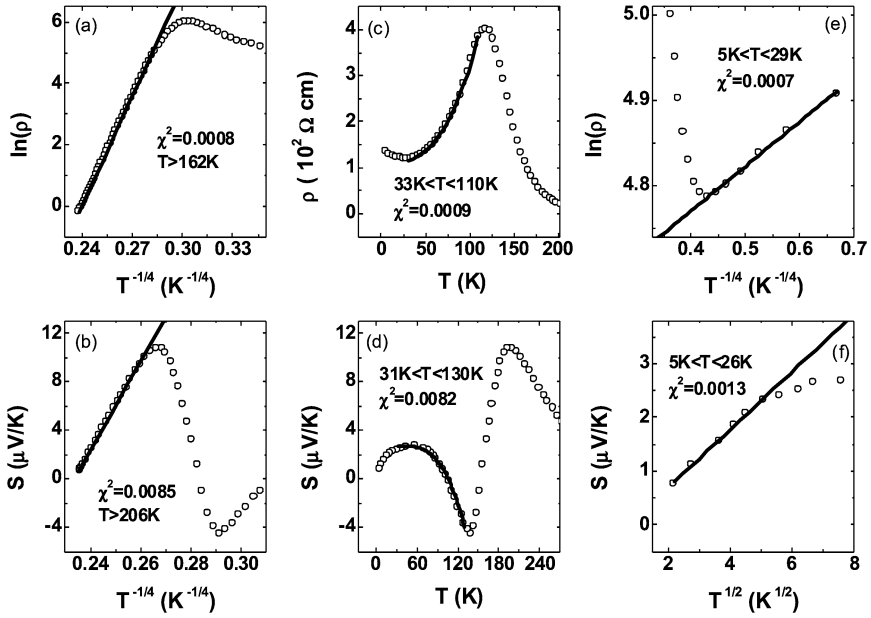

Fig. 5. (a) The plot of $\ln\rho$ against $T^{-1/4}$ and (b) S vs. $T^{-1/4}$ in the high-temperature PM insulating region. (c) The plot of ρ vs. T and (d) S vs. T in the intermediate-temperature FM metallic region. (e) The plot of $\ln\rho$ against $T^{-1/4}$ and (f) S vs. $T^{1/2}$ in the low-temperature FM insulating region, respectively. The solid lines are the fitting data. The parameter χ^2 stands for the quality of the fitting.

local distortion of MnO_6 octahedra has such an ability lifting the degenerate e_g band. Whereas, the thermally induced and the field-induced sign change of S below T_C would be difficult to be interpreted because the JT effect can be less prominent or vanished in the FM state [13].

Another possible origin can be related to the antiferromagnetic (AFM) orbital ordering in the FM ground state. For the $La_{0.85}Te_{0.15}Mn_{0.9}Cu_{0.1}O_3$ sample, the distinct discrepancy of zero-field cooling (ZFC) magnetization and field cooling (FC) magnetization below a freezing point temperature is observed, indicating that the spin-glass-like behavior probably occurs due to the competition between AFM and FM interaction [5]. That is to say, there exists AFM background at low temperatures. Due to the full spin polarization of the e_g band, the spin degree of freedom is lost and only the orbital degree of freedom survives in the FM ground state. Therefore, the behavior of full spin polarization in terms of a change of electronic structure can be relate to the orbital degree of freedom of the e_g carriers in the AFM ordering.

Additionally, in the high-temperature PM insulating region above T_C, $\rho(T)$ and $S(T)$ data at zero field and external field can be fitted well by three-dimensional Mott's variable-range-hopping (VRH) model, $\rho(T) = \rho_0 \exp[(T_0/T)^{1/4}]$ [7], with $T_0 \approx 21/[k_B N(E_F)\xi^3]$, where ξ is the localization length, $N(E_F)$ is the density of localized states at the Fermi energy, and $S(T) \propto (\frac{T_{0S}}{T})^{1/4}$ [15], T_{0S} is the characteristic temperature similar to the temperature T_0 of the VRH formula of $\rho(T)$. The plot of $\ln\rho(T)$ vs. $T^{-1/4}$ and S against $T^{-1/4}$ at zero field are shown in Fig. 5(a), (b), respectively. The scatter symbols correspond to the experimental data and the solid lines denote the fitted results according to Mott's VRH model. The fitting parameter values of $T_{0\rho}^H$ and T_{0S}^H (denoting the values of T_0 and T_{0S} in the high-temperature region obtained by fitting $\rho(T)$ and $S(T)$ data) are listed in Table 1. The large values of characteristic temperature $T_{0\rho}^H$ and T_{0S}^H at zero field imply the strong localization length ξ provided the density of state $N(E_F)$ at the Fermi level does not change. Additionally, it is clearly seen that the applied field reduces the values of $T_{0\rho}^H$ and T_{0S}^H, which is suggested to be related to the delocalization e_g^1 electron of Mn^{3+} ions.

Table 1
The fitting parameters of $La_{0.85}Te_{0.15}Mn_{0.9}Cu_{0.1}O_3$ sample. The definition of $T_{0\rho}^H$, T_{0S}^H, ρ_0, $\rho_{2.5}$, S_0, $S_{3/2}$, S_4, $T_{0\rho}^L$, and A is denoted in text, respectively. "±" expresses the error produced by fitting $\rho(T)$ and $S(T)$ data

Parameter	0 T	4 T
$(T_{0\rho}^H)^{1/4}$ ($K^{1/4}$)	118.37 ± 0.41	106.69 ± 0.48
$(T_{0S}^H)^{1/4}$ ($K^{1/4}$)	368.84 ± 0.58	324.66 ± 0.45
ρ_0 (Ω cm)	102.0516 ± 0.0325	94.3156 ± 0.0142
$\rho_{2.5}$ (Ω cm/$K^{2.5}$)	$(2.2732 \pm 0.0213) \times 10^{-3}$	$(8.7654 \pm 0.0035) \times 10^{-4}$
S_0 (μV/K)	1.99 ± 0.07	0.54 ± 0.10
$S_{3/2}$ (μV/$K^{5/2}$)	$(3.04 \pm 0.05) \times 10^{-3}$	$(3.76 \pm 0.05) \times 10^{-3}$
S_4 (μV/K^5)	$(-4.81 \pm 0.05) \times 10^{-9}$	$(-5.36 \pm 0.06) \times 10^{-9}$
$(T_{0\rho}^L)^{1/4}$ ($K^{1/4}$)	0.52 ± 0.02	0.44 ± 0.02
A (μV/$K^{3/2}$)	0.38 ± 0.01	0.32 ± 0.03

In the intermediate-temperature FM metallic region below T_C, the present $\rho(T)$ data for the sample can well meet the equation $\rho = \rho_0 + \rho_{2.5}T^{2.5}$ [16], where the temperature independent term ρ_0 is the resistivity caused by domain, grain boundary and other temperature independent scattering mechanisms, the $\rho_{2.5}T^{2.5}$ term which represents a combination of electron–electron, electron–phonon and electron–magnon scattering [17]. Fig. 5(c) shows the curves of ρ vs. T at zero field for the sample. The fitting parameters values of ρ_0 and $\rho_{2.5}$ are listed in Table 1. The reduction of both ρ_0 and $\rho_{2.5}$ in

the applied field is attributed to the decreased magnetic domain boundaries and the suppressed spin fluctuation in the FM metallic phase, respectively. In general, the transport mechanism should be determined by $\rho(T)$ and $S(T)$ data together. Similar to $\rho(T)$ data, several factors such as impurity, complicated band structure, electron–electron, electron–magnon scattering, etc., affect $S(T)$ data in the FM metallic region. It is reasonable to assume that the $\rho(T)$ and $S(T)$ data are closely related to the similar transport mechanism. So far, the temperature dependence of $S(T)$ data in this intermediate-temperature FM region has been analyzed by the equation $S = S_0 + S_{3/2}T^{3/2} + S_4T^4$ [6], where S_0 (defined from the value of S at $T = 0$ K) is inserted to account for the problem truncating the low-temperature data, and the $T^{3/2}$ dependence is attributed to electron–magnon scattering process. The origin of the S_4T^4 term may be due to the spin-wave fluctuation in the FM phase as argued in Ref. [18]. The fitting parameters corresponding to $H = 0$ and 4 T are listed in Table 1, respectively. Firstly, we can clearly see that $S_{3/2}$ is nearly six orders of magnitude larger than that of S_4, implying the second term $S_{3/2}T^{3/2}$ dominates the transport mechanism in the FM metallic region below T_C. Secondly, based on Fig. 5(c), (d), it exhibits that the fitting temperature range by $S(T)$ measurement is close to that of $\rho(T)$ measurement, indicating that the transport mechanism can be suggested to originate from electron–magnon scattering. When a magnetic field is applied, the effect of field inducement on the magnon scattering enhances. Actually, similar transport mechanism of electron–magnon scattering is also observed in $LaMnO_3$ [6] and $La_{0.5}Pb_{0.5}Mn_{1-x}Cr_xO_3$ [18] system.

In the low-temperature FM insulating region, it is found that Mott's 3D VRH model matches the $\rho(T)$ and $S(T)$ data well, $S(T)$ in the limit of $T \to 0$ meets the relationship $|S| = A(T)^{1/2} + B$ [19], where A is a factor determined by the density of state in the vicinity of Fermi surface $N(E_F)$, B is a constant. The curves of $\ln\rho(T)$ against $T^{-1/4}$ and S vs. $T^{1/2}$ for the sample are plotted in Fig. 5(e) and (f), respectively. The fitting parameters $T_{0\rho}^L$ (denoting the values of T_0 in the low-temperature region obtained by fitting $\rho(T)$ data) and A are listed Table 1. The small values of $T_{0\rho}^L$ and A is suggested to stem from the weak carrier localization as mentioned above. As to the reduction of $T_{0\rho}^L$ and A in the applied field, it is attributed to the delocalization of the carrier caused by the applied field.

In a word, from the above results, it is found that the $La_{0.85}Te_{0.15}Mn_{0.9}Cu_{0.1}O_3$ sample plays a crucial role to determine the transport properties. The observed changes are strongly related to the spin polarization because of the interesting variation of sign on S. Furthermore, the transport mechanism has been determined in the different temperature region. Such results also reflect the special role of $La_{0.85}Te_{0.15}Mn_{0.9}Cu_{0.1}O_3$ sample. At the same time, it can also help us to improve our understanding to other complex systems.

4. Conclusions

In summary, both $\rho(T)$ and $S(T, H)$ of the $La_{0.85}Te_{0.15}Mn_{0.9}Cu_{0.1}O_3$ sample have been measured in the absence and presence of magnetic fields. A large negative MR is observed at 5 T. The $S(T)$ shows an anomalous peak, which can be related to phonon drag effect. The sign variation of S induced by the temperature and the applied magnetic field is observed. We suggest that the sign variation of S may be related to the spin polarization. According to the change of electronic structure, the orbital degree of freedom of the e_g carriers can be responsible for these behaviors. Based on the results of $\rho(T)$ and $S(T)$, the transport mechanism in the high-temperature PM region and low-temperature FM insulating region below T_C for the sample can be described by VRH conduction. However, in the intermediate-temperature FM metallic region below T_C, $\rho(T)$ and $S(T)$ of the sample are well fitted by the formula: $\rho = \rho_0 + \rho_{2.5}T^{2.5}$ and $S = S_0 + S_{3/2}T^{3/2} + S_4T^4$, respectively, implying the importance of electron–magnon scattering.

Acknowledgements

This work is supported by the National Key Basic Research under Contract No. 001CB610604, and the National Nature Science Foundation of China under Contract No. 10474100 and Director's Fund of Hefei Institutes of Physical Science, Chinese Academy of Sciences.

References

[1] S. Jin, T.H. Tiefel, M. McCormack, R.A. Fastnacht, R. Ramesh, L.H. Chen, Science 264 (1994) 413;
A. Asamitsu, Y. Moritomo, Y. Tomioka, T. Arima, Y. Tokura, Nature (London) 373 (1995) 407;
R. von Helmolt, J. Wecker, B. Holzapfel, L. Schultz, K. Samwer, Phys. Rev. Lett. 71 (1993) 2331.
[2] C. Zener, Phys. Rev. 82 (1951) 403.
[3] J.B. Goodenough, Phys. Rev. 100 (1955) 564.
[4] P. Mandal, S. Das, Phys. Rev. B 56 (1997) 15073;
S. Roy, N. Ali, J. Appl. Phys. 89 (2001) 7425;
G.T. Tan, S.Y. Dai, P. Duan, Y.L. Zhou, H.B. Lu, Z.H. Chen, Phys. Rev. B 68 (2003) 014426.
[5] J. Yang, W.H. Song, Y.Q. Ma, R.L. Zhang, B.C. Zhao, Z.G. Sheng, G.H. Zheng, J.M. Dai, Y.P. Sun, Phys. Rev. B 70 (2004) 092504.
[6] P. Mandal, Phys. Rev. B 61 (2000) 14675.
[7] N.F. Mott, E.A. Davis, in: Electronic Processes in Non-Crystalline Materials, Clarendon, Oxford, 1971.
[8] S. Uhlenbruck, B. Buchner, R. Gross, A. Freimuth, A. Maria de Leon Guevara, A. Revcolevschi, Phys. Rev. B 57 (1998) 5571.
[9] A. Asamitsu, Y. Moritomo, Y. Tokura, Phys. Rev. B 53 (1996) 2952.
[10] R.D. Barnard, Thermoelectricity in Metals and Alloys, Taylor & Francis, London, 1972.
[11] F.J. Blatt, P.A. Schroeder, C.L. Foiles, D. Greig, Thermoelectric Power of Metals, Plenum, New York, 1976.
[12] C. Mitra, P. Raychaudhuri, K. Dörr, K.-H. Müller, L. Schultz, P.M. Oppeneer, S. Wirth, Phys. Rev. Lett. 90 (2003) 017202.
[13] A.J. Millis, P.B. Littlewood, B.I. Shraiman, Phys. Rev. Lett. 74 (1995) 5144.
[14] H.Y. Hwang, S.-W. Cheong, P.G. Radaelli, M. Marezio, B. Batlogg, Phys. Rev. Lett. 75 (1995) 914.
[15] I.P. Zvyagin, Fiz. Tekh. Poluprovodn. (St. Peterburg) 12 (1978) 1018.
[16] J.M. De Teresa, M.R. Ibarra, J. Blasco, J. García, C. Marquina, P.A. Algarabel, Z. Arnold, K. Kamenev, C. Ritter, R. von Helmolt, Phys. Rev. B 54 (1996) 1187.
[17] P. Schiffer, A.P. Ramirez, W. Bao, S.W. Cheong, Phys. Rev. Lett. 75 (1995) 3336.
[18] A. Banerjee, S. Pal, S. Bhattacharya, B.K. Chauhuri, H.D. Yang, Phys. Rev. B 64 (2001) 104428.
[19] I.P. Zvyagin, Phys. Status Solidi B 58 (1973) 443;
H. Overhof, Phys. Status Solidi B 67 (1975) 709.